Electronic Supplementary Material (ESI) for Journal of Materials Chemistry A.
This journal is © The Royal Society of Chemistry 2020

Supporting Information

Degradation mechanisms in mixed-cation and mixed-halide $Cs_xFA_{1-x}Pb(Br_yI_{1-y})_3$ perovskite films under ambient conditions

*Paulo Ernesto Marchezi[a], Eralci Moreira Therézio[a,b], Rodrigo Szostak[a], Hugo Campos Loureiro[a], Karsten Bruening[c], Aryeh Gold-Parker[c], Maurício A. Melo Jr.[d], Christopher J. Tassone[c], Helio C. N. Tolentino[e], Michael F. Toney[c] and Ana Flávia Nogueira[*a]*

[a.] *Chemistry Institute, University of Campinas, Campinas, SP, Brazil.*

[b.] *Physics Institute, Federal University of Mato Grosso, Cuiabá, MT, Brazil.*

[c.] *Stanford Synchrotron Radiation LightSource (SSRL), Menlo Park, California, USA.*

[d.] *São Carlos Institute of Physics, University of São Paulo, 13560-970, São Carlos, SP, Brazil.*

[e.] *Brazilian Synchrotron Light Laboratory (LNLS), Brazilian Center for Research in Energy and Materials (CNPEM), Campinas, SP 13083-970, Brazil.*

**Corresponding author:* anafla@unicamp.br

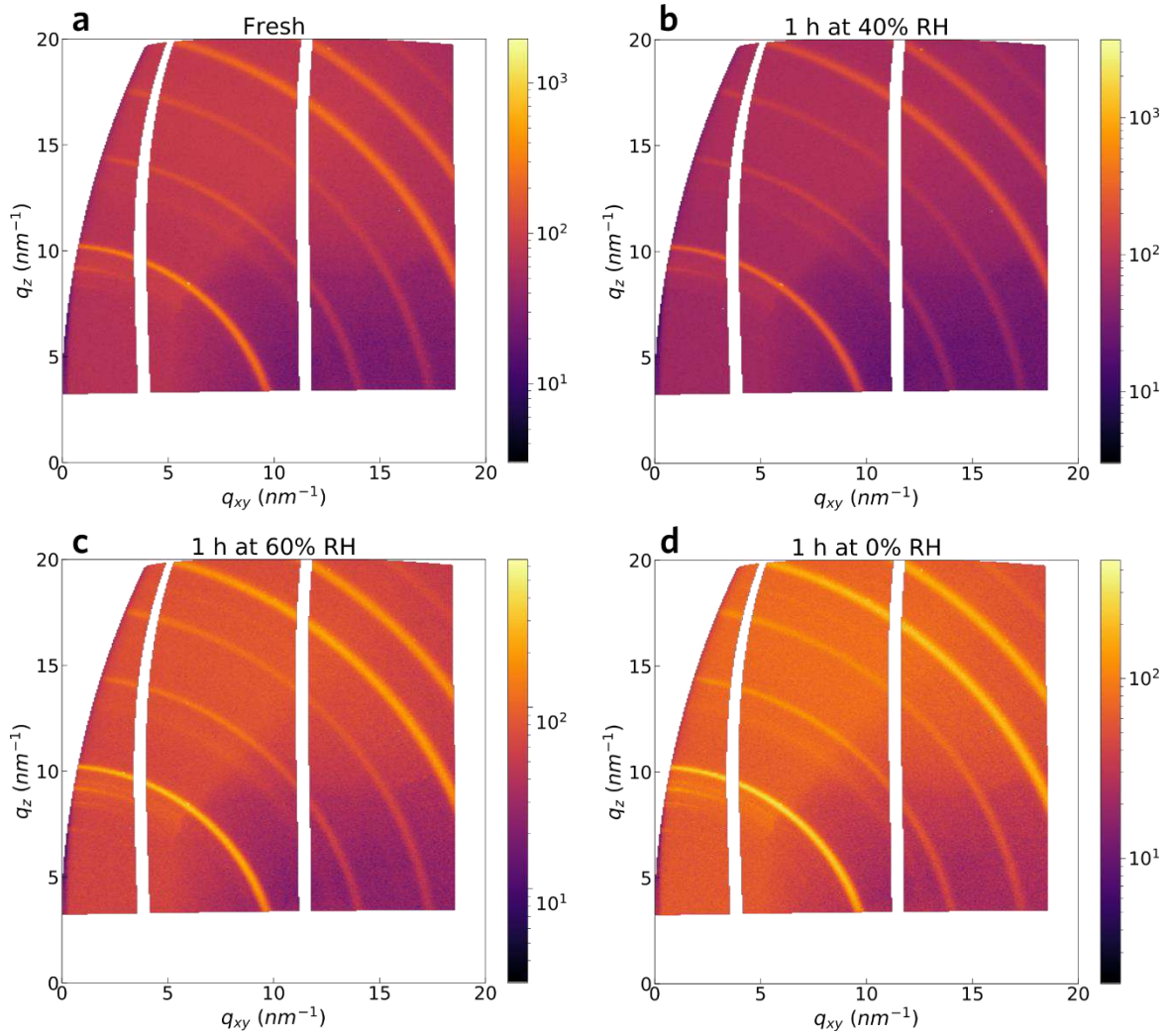

Figure S 1: GIWAXS reciprocal lattice maps related to the 1D profiles in Figure 1a and 1b (sample 10/17). Fresh (a), after 1 h at 40% RH (b), after 1 h at 60% RH (c) and after 1 h back to 0% RH (d).

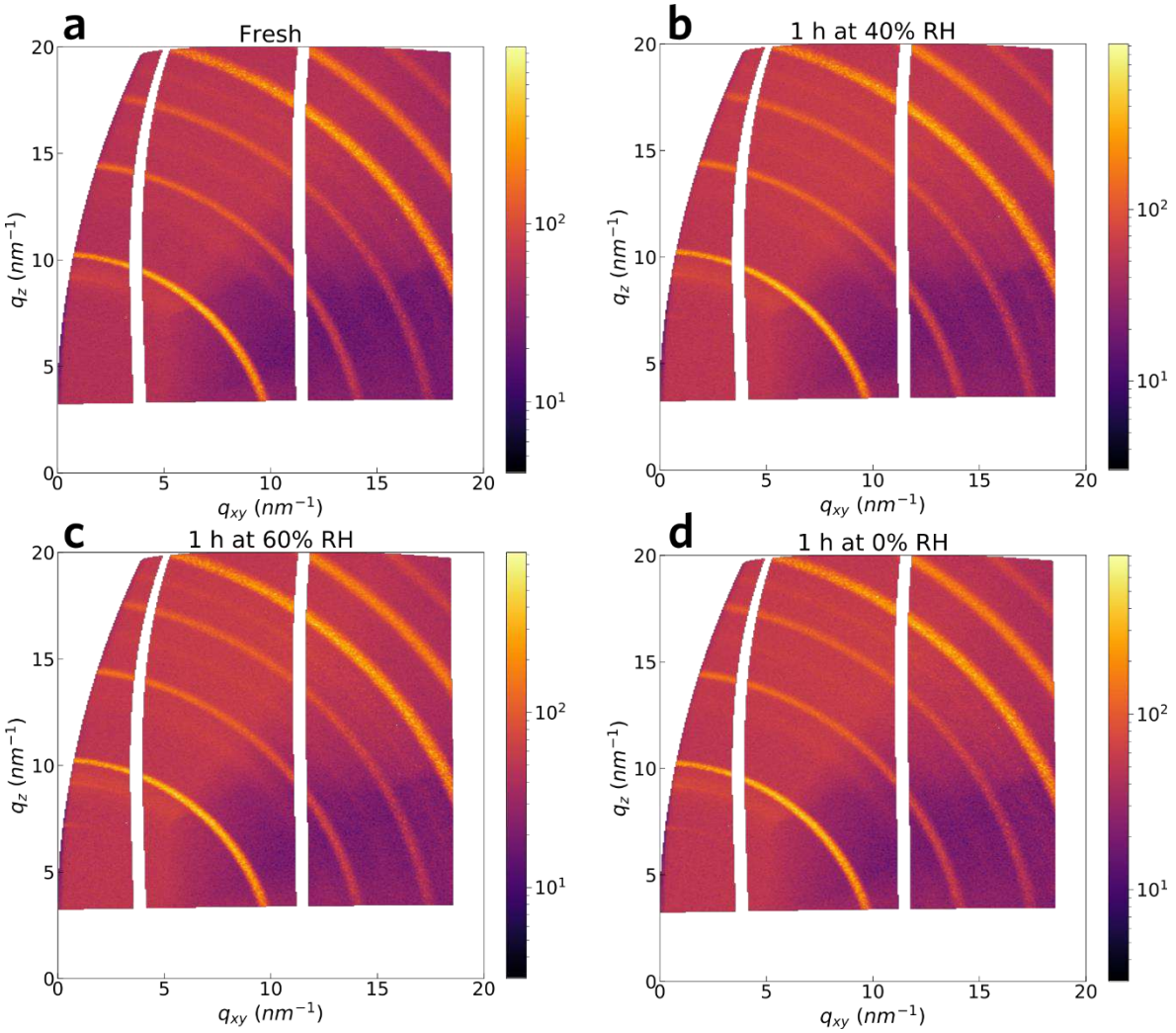

Figure S 2: GIWAXS reciprocal lattice maps related to the 1D profiles in Figure 1a and 1c (sample 20/17). Fresh (a), after 1 h at 40% RH (b), after 1 h at 60% RH (c) and after 1 h back to 0% RH (d).

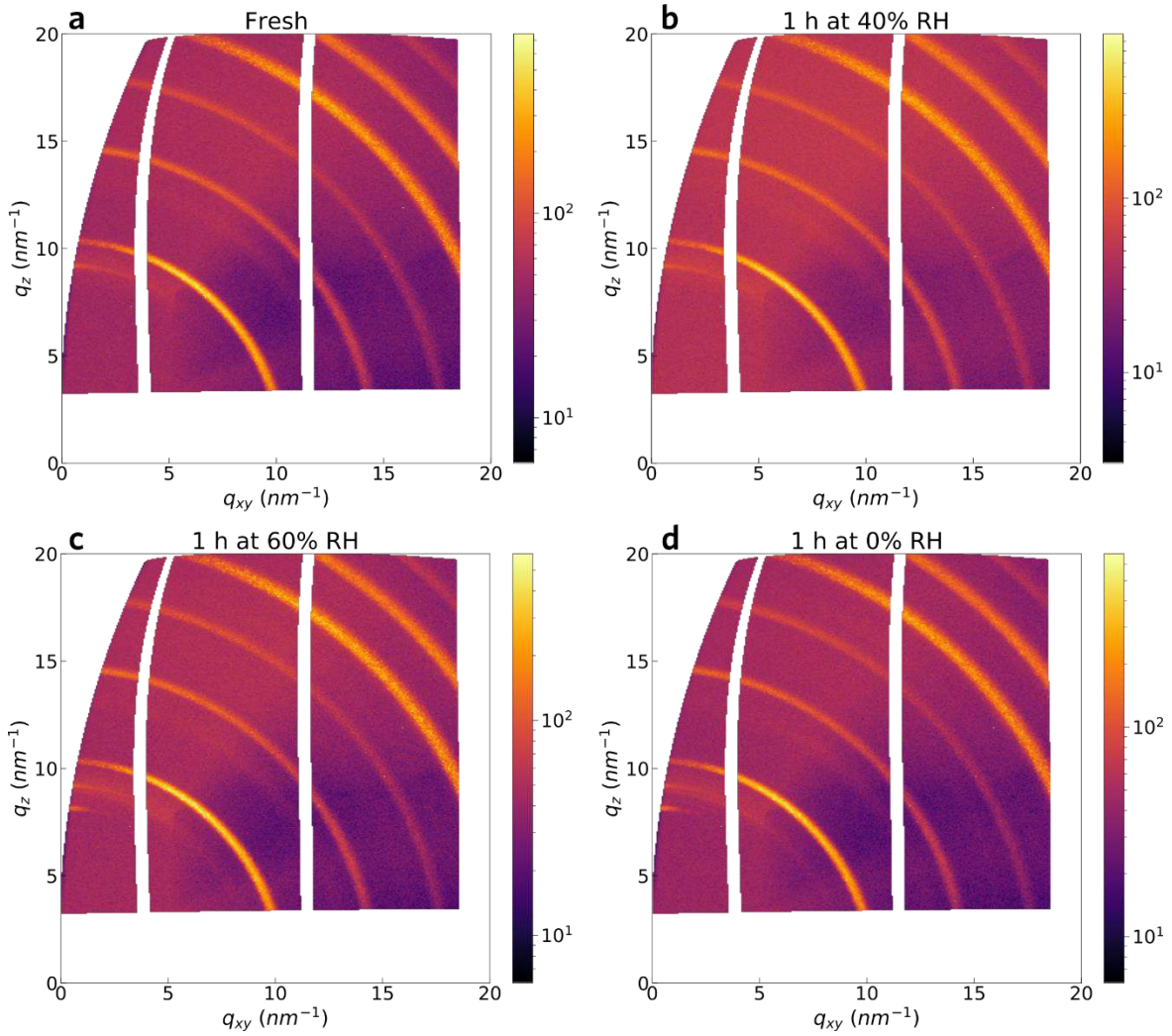

Figure S 3: GIWAXS reciprocal lattice maps related to the 1D profiles in Figure 1a and 1d (sample 10/38). Fresh (a), after 1 h at 40% RH (b), after 1 h at 60% RH (c) and after 1 h back to 0% RH (d).

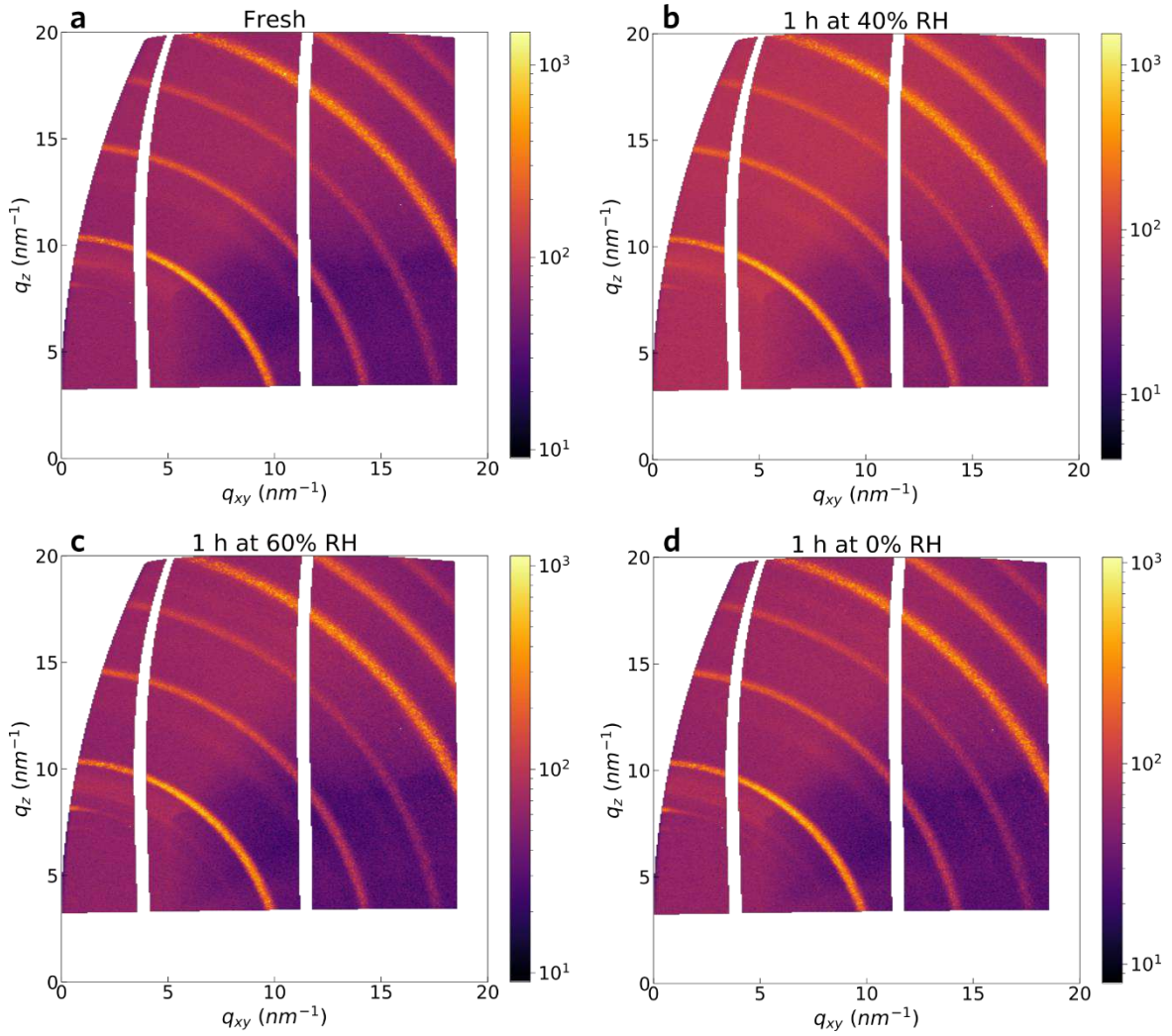

Figure S 4: GIWAXS reciprocal lattice maps related to the 1D profiles in Figure 1a and 1f (sample 20/38). Fresh (a), after 1 h at 40% RH (b), after 1 h at 60% RH (c) and after 1 h back to 0% RH (d).

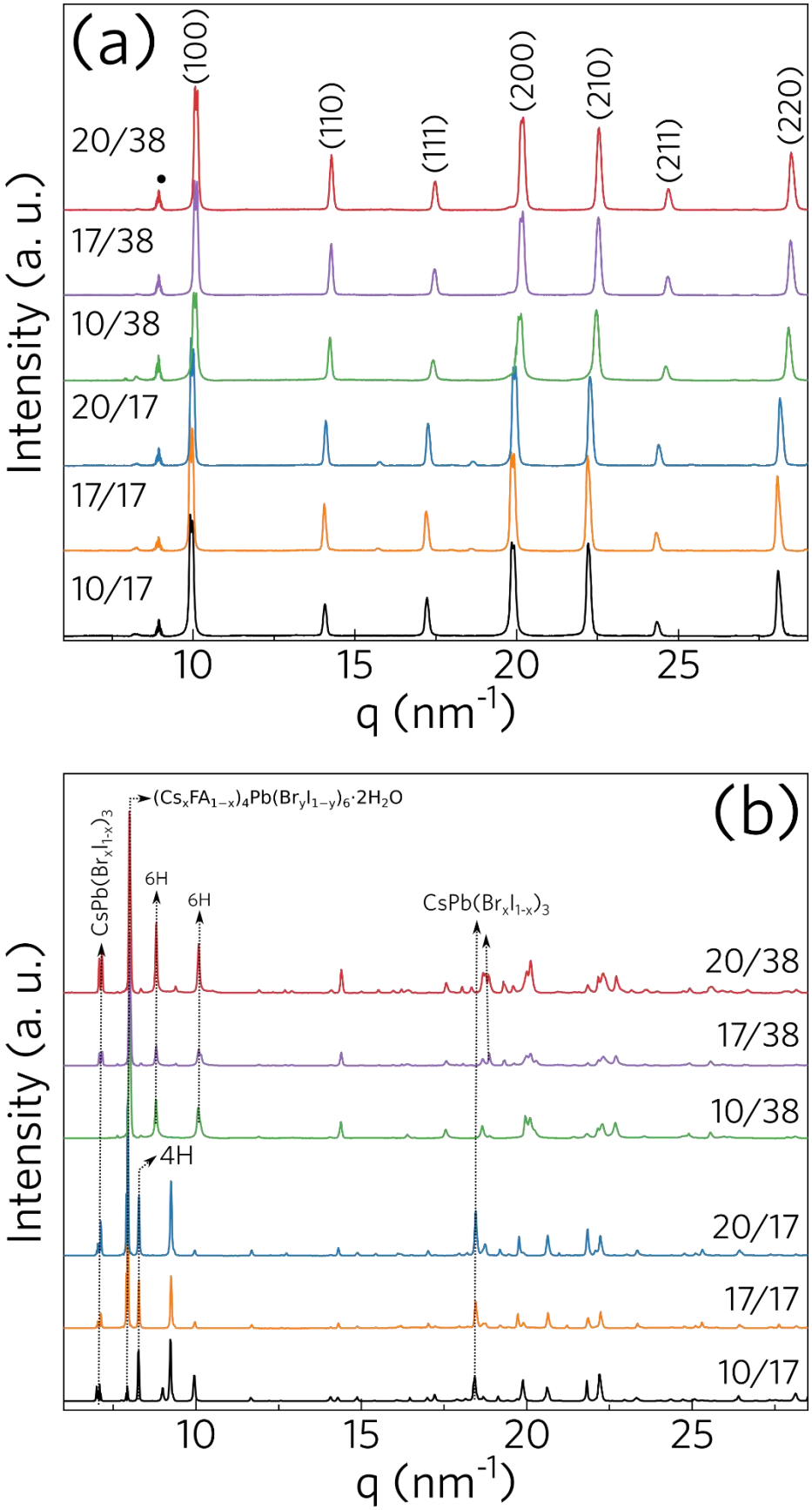

Figure S 5: (a) XRD pattterns taken before and (b) all range of the XRD presented in Figure 2 (after degradation). The reciprocal lattice maps for all the 1D profiles in (a) and (b) are presented in Figure S6 and Figure S7, respectively.

Table S 1: Attribution of diffractograms peaks of Figure S7.

$Cs_yFA_{(1-y)}Pb(Br_xI_{(1-x)})_3$ after degradation	
Peak *(q / nm^{-1})*	Attribution
***6.9*, 7.1**	δ-$CsPbX_3$ (orthorhombic) [1]
8	$(Cs_xFA_{1-x})_4Pb(Br_yI_{1-y})_6 \cdot 2H_2O$ [1], [2]
8.2, 9.2	4H phase [1]
8.7, 9.9	6H phase [1]
9.9-10.1	6H and 3R/3C phases [1]
11.6	PbO
12.3	$PbBr_2$ (110) [3], [4]
12.1, 12.4, 18,5	δ Yellow Delta Phase (orthorhombic) [2] ($CsPbX_3$)
18.9	CsI [5]
21.7-22.7	$Cs_xFA_{1-x}Pb(Br_yI_{1-y})_3 \cdot H_2O$ and $(Cs_xFA_{1-x})_4Pb(Br_yI_{1-y})_6 \cdot 2H_2O$ [1], [2]
24.4	$CsPbX_3$ [5]
26.1	$PbBr_2$ [2]

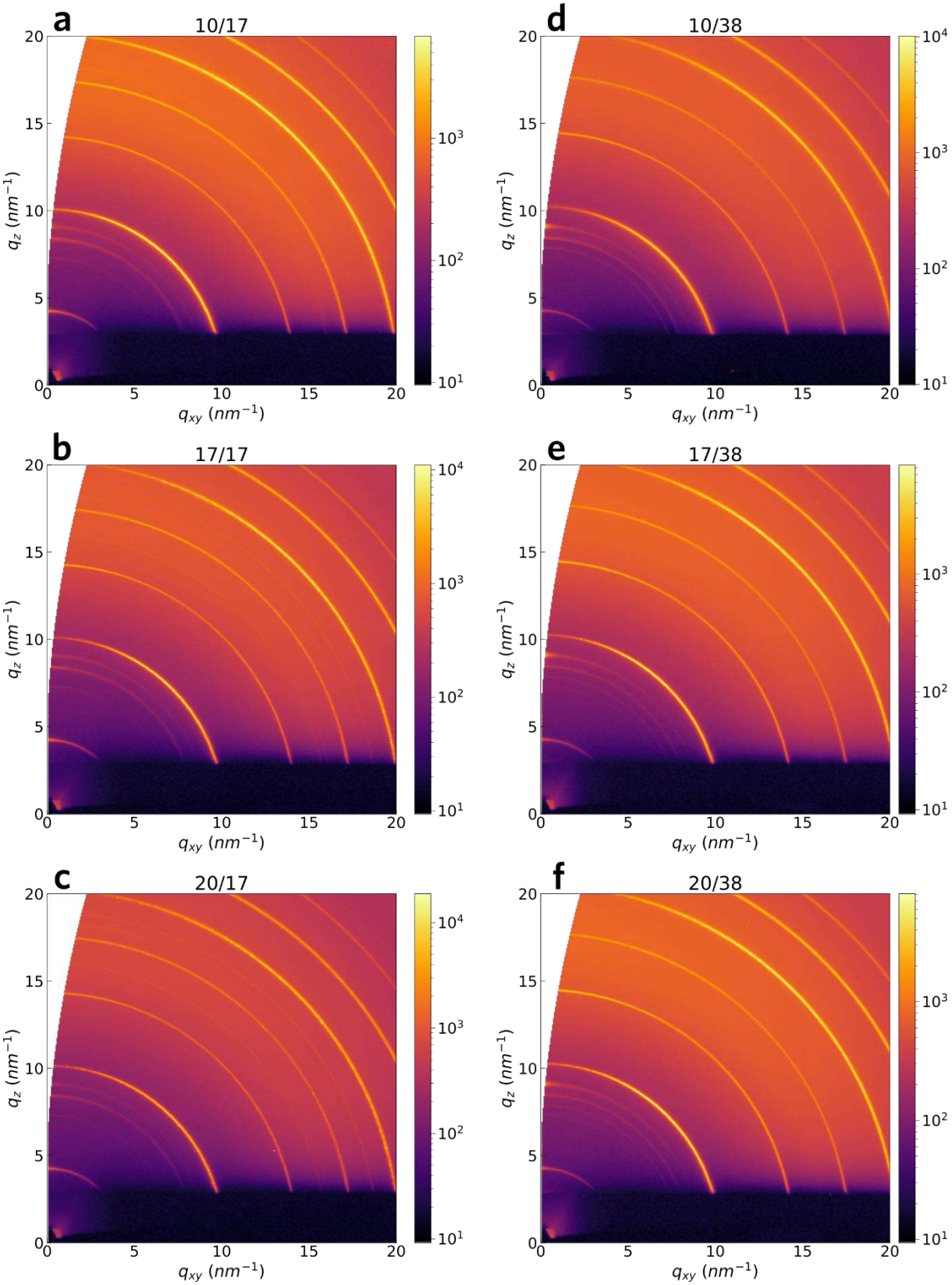

Figure S 6: GIWAXS reciprocal lattice maps of all the XRD presented in Figure S5(a). Pristine 10/17 (a), pristine 17/17 (b), pristine 20/17 (c), pristine 10/38(d), pristine 17/38 (e) and pristine 20/38 (f).

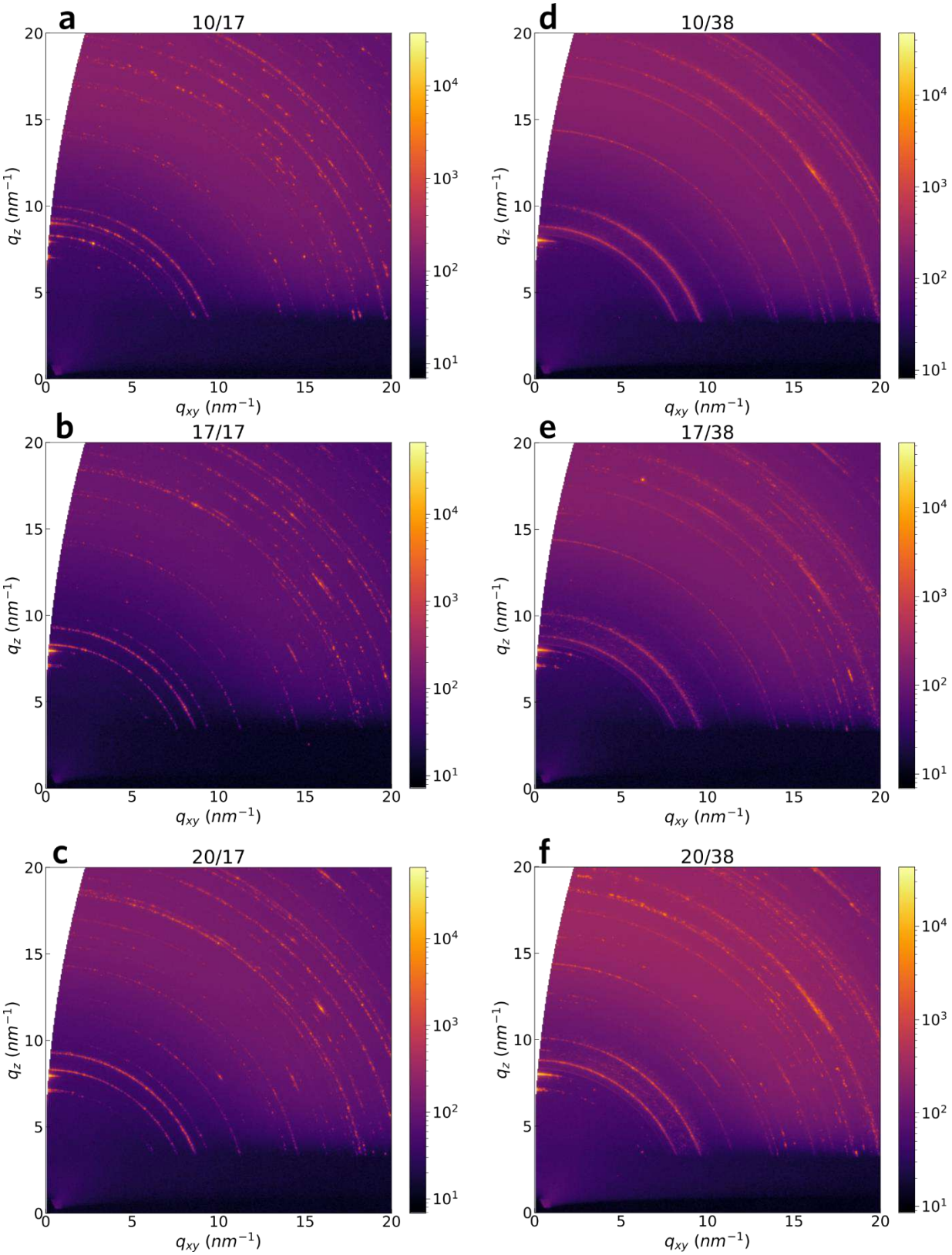

Figure S 7: GIWAXS reciprocal lattice maps of all the XRD presented in Figure S5(b) and Figure 2. Degraded10/17 (a), degraded 17/17 (b), degraded 20/17 (c), degraded 10/38(d), degraded 17/38 (e) and degraded 20/38 (f).

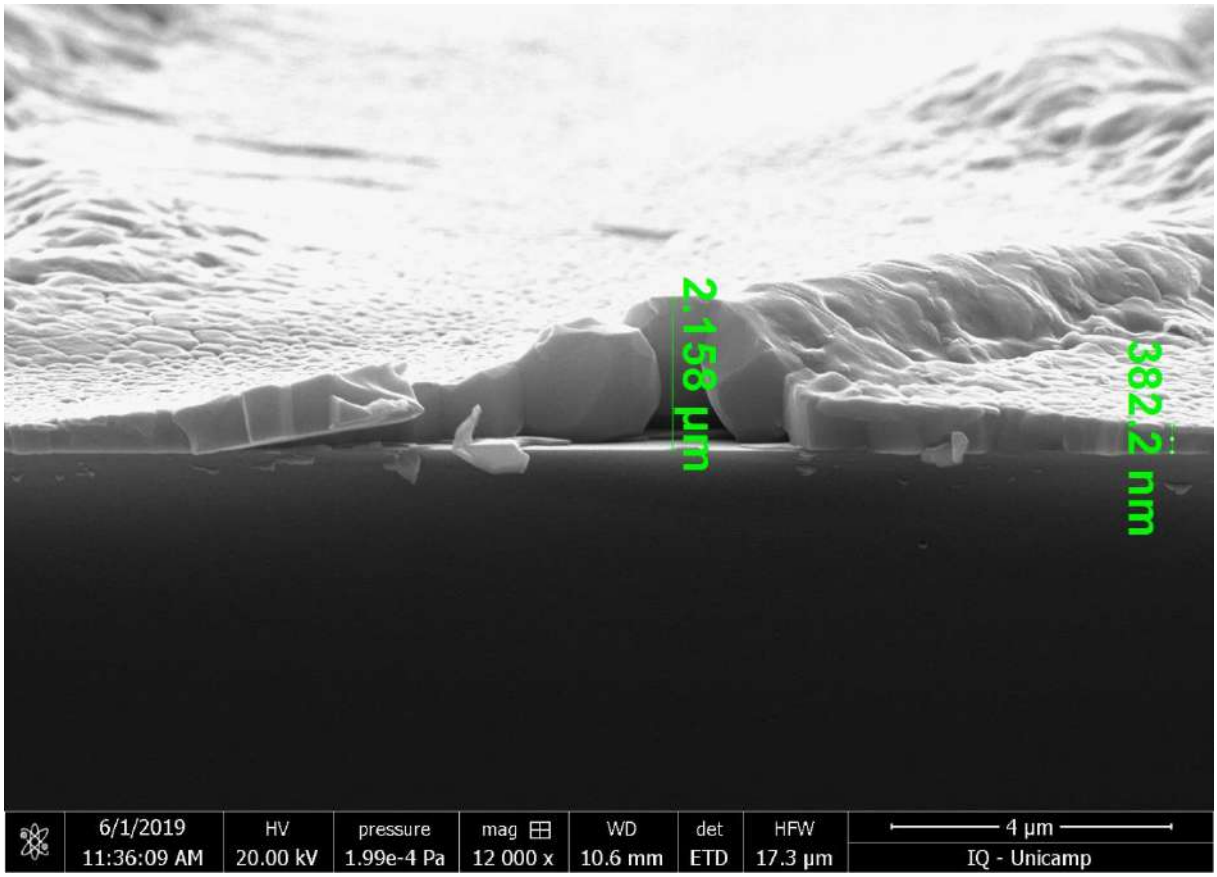

Figure S 8: Cross section SEM image of sample 17/17.

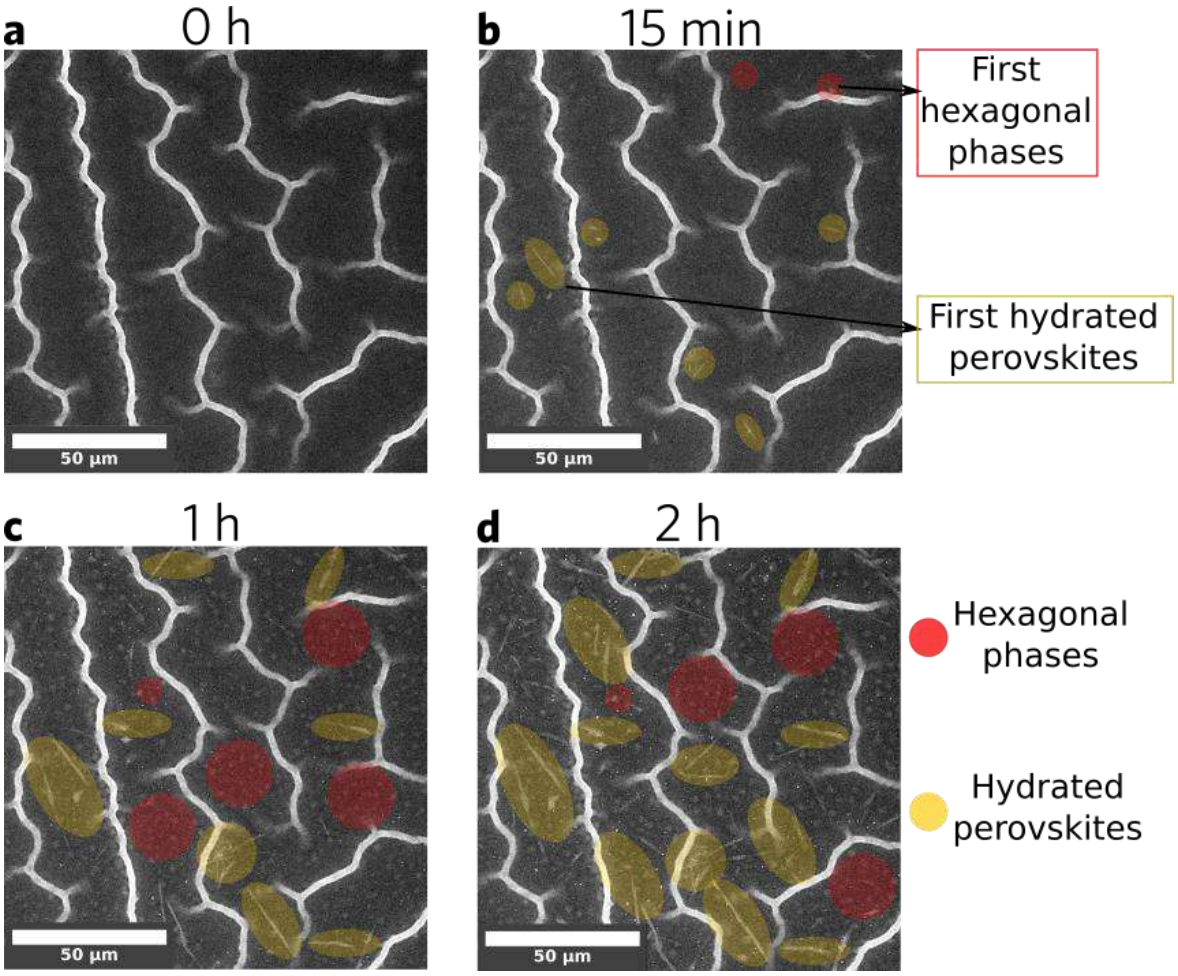

Figure S 9: In-situ FEG-ESEM images during degradation of sample 10/38 upon humidity exposion (75 %rH). (a) fresh sample, (b) 15 min, (c) 1 h, (d) 2 h. See the Supporting Videos for a real-time visualization.

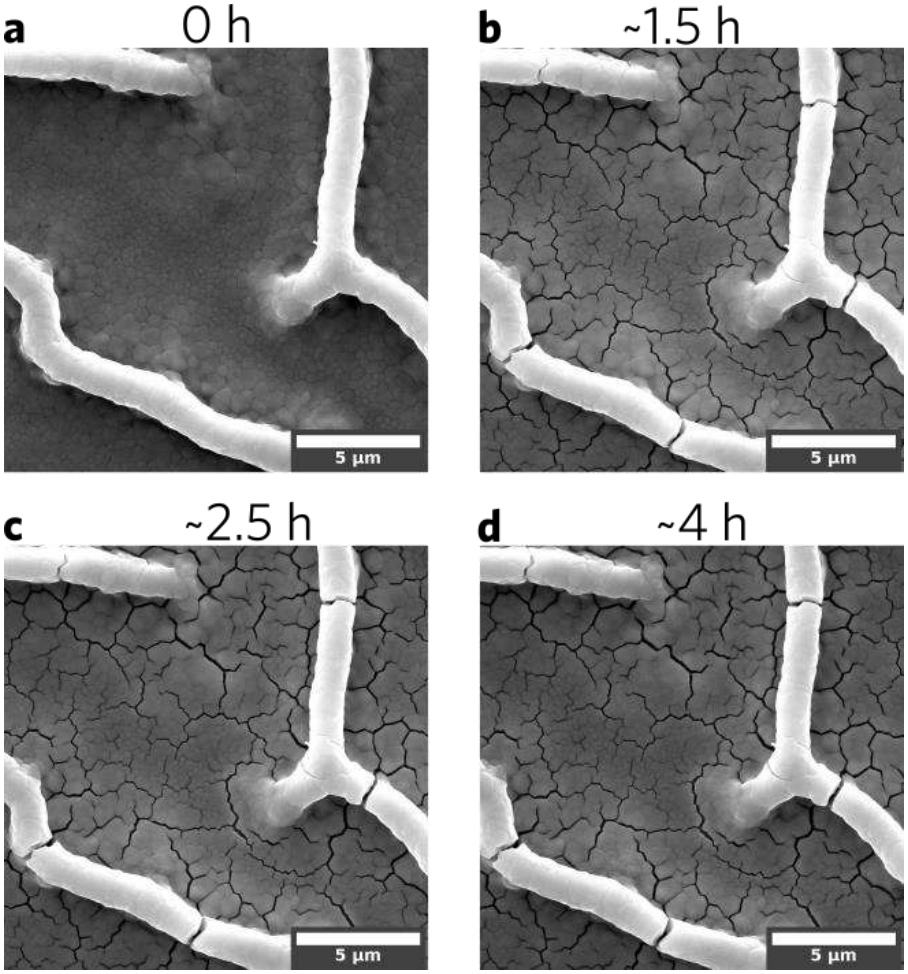

Figure S 10: In-situ FEG-SEM in high-vacuum mode. (a) fresh sample, (b) ~1.5 h, (c) ~2.5 h, (d) ~4 h. See the Supporting Videos for a real-time visualization.

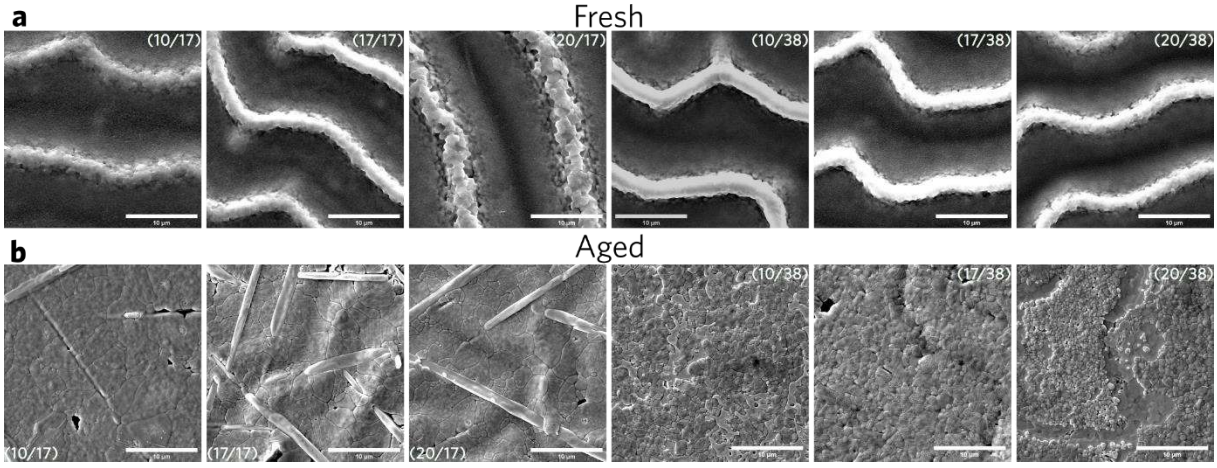

Figure S 11: SEM images of samples 10/17, 17/17, 20/17, 10/38, 17/38 and 20/38 before (a) and after degradation (b).

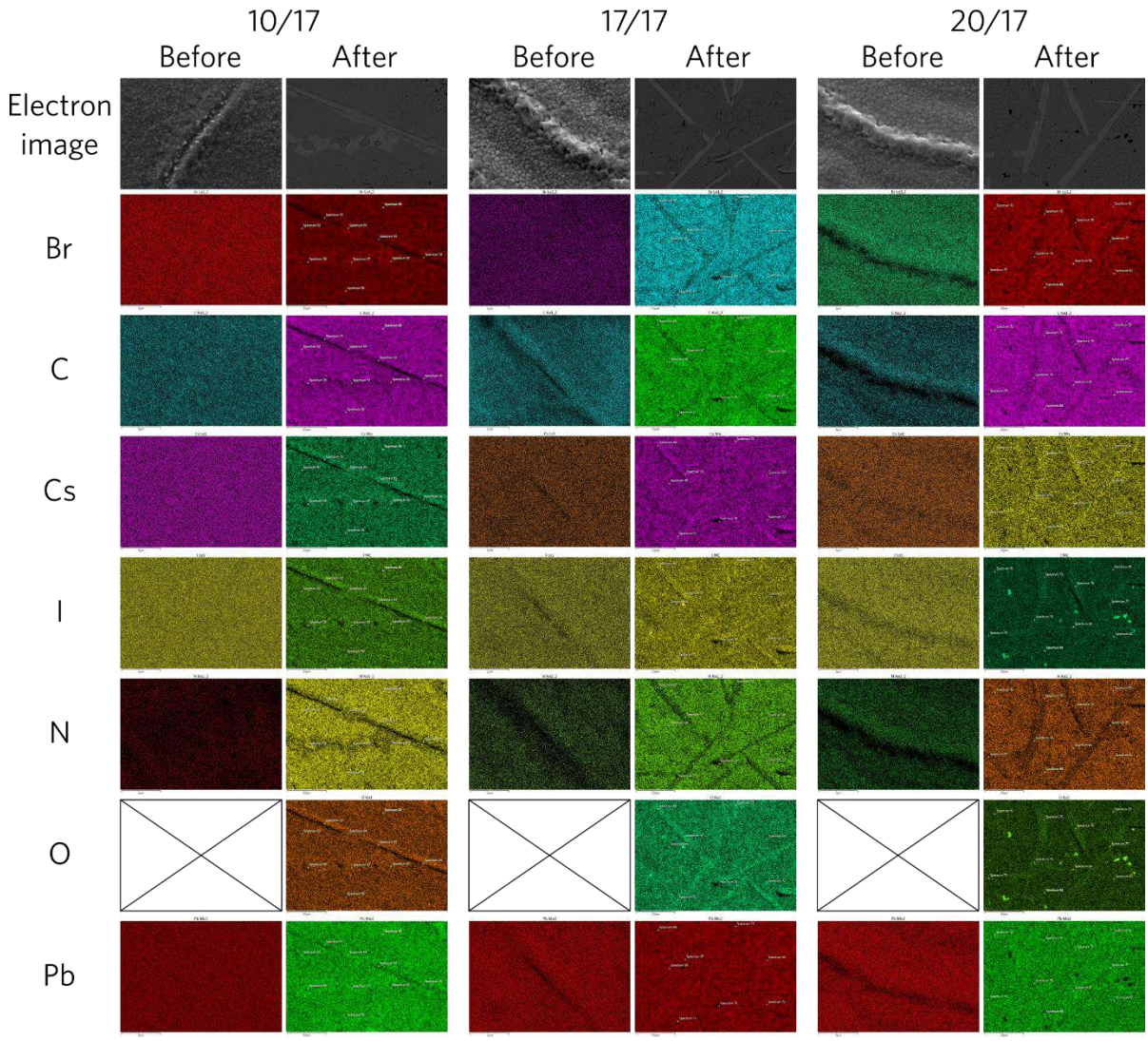

Figure S 12: EDS maps of Br, C, Cs, I, N, O and Pb for samples 10/17, 17/17 and 20/17, before and after degradation.

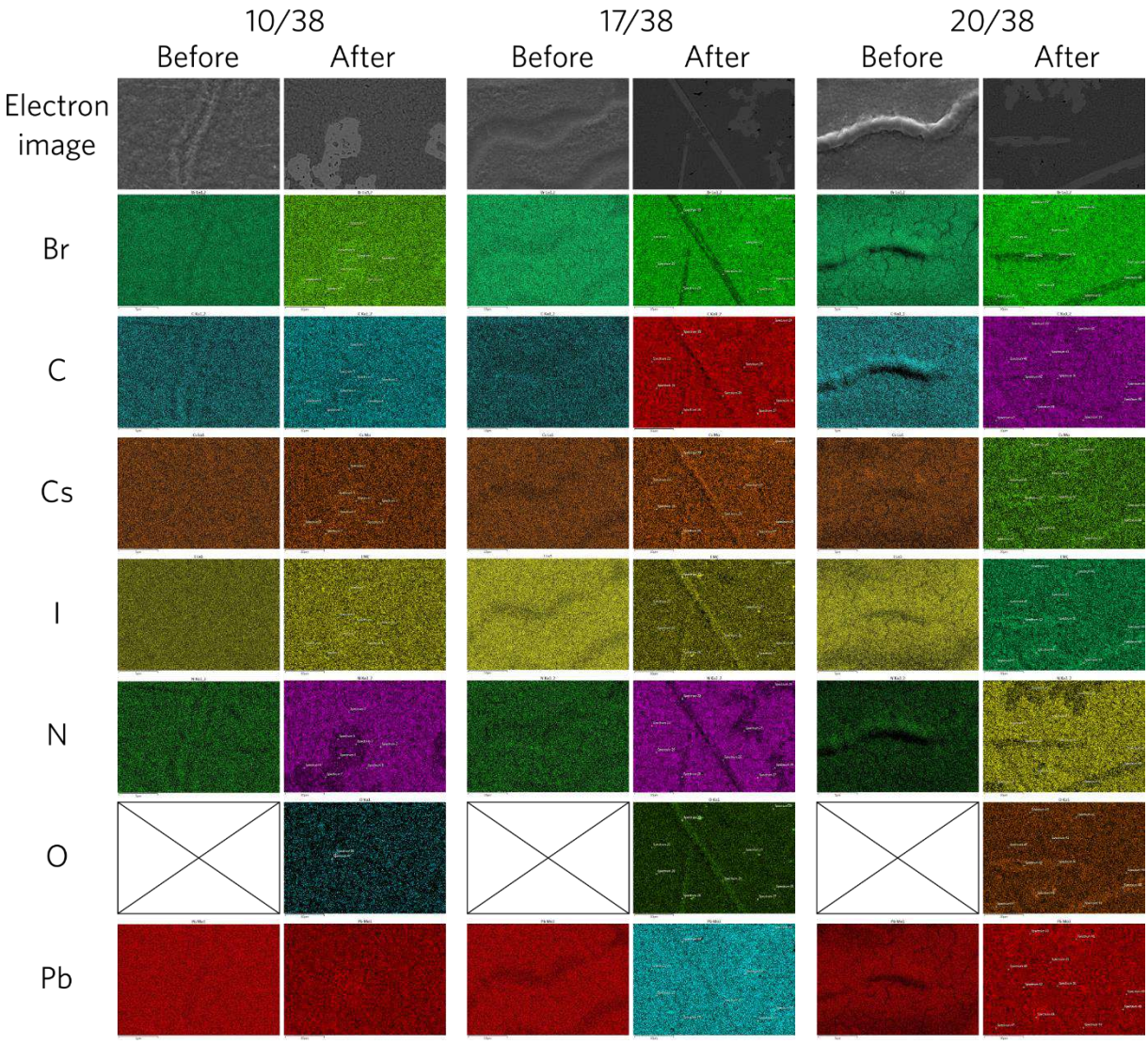

Figure S 13: EDS maps of Br, C, Cs, I, N, O and Pb for samples 10/38, 17/38 and 20/38, before and after degradation.

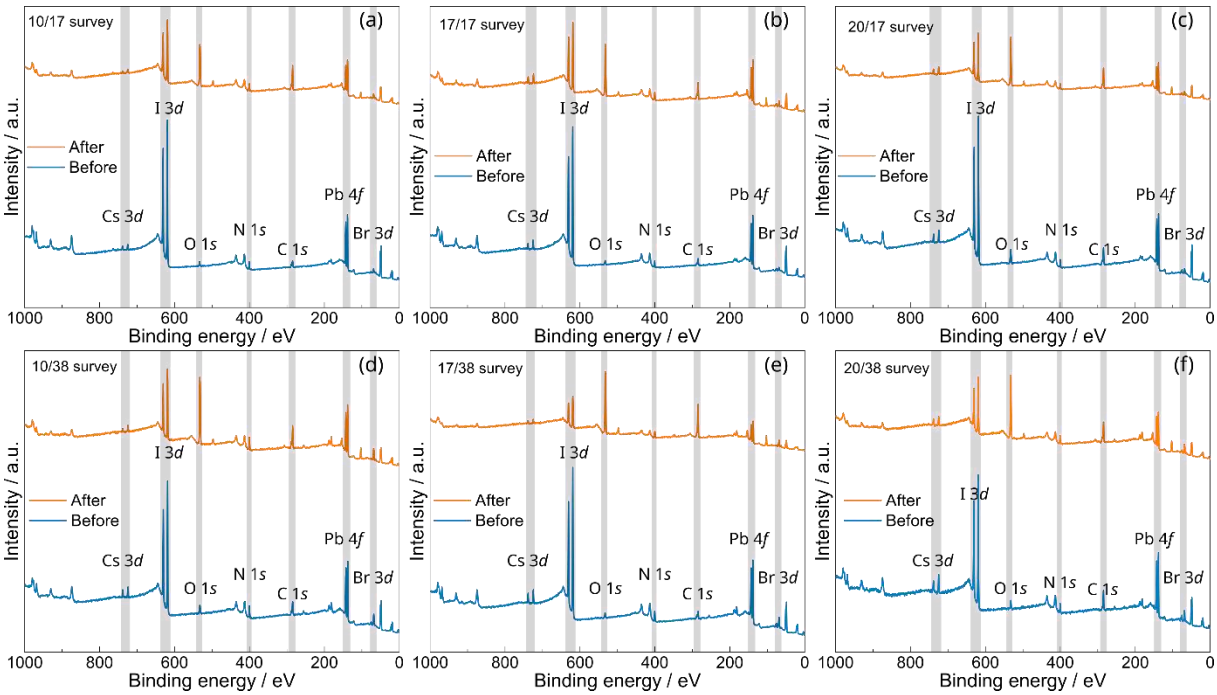

Figure S 14: Before and after degradation XPS survey scan of samples 10/17 (a), 17/17 (b), 20/17 (c), 10/38 (d), 17/38 (e) and 20/38 (f).

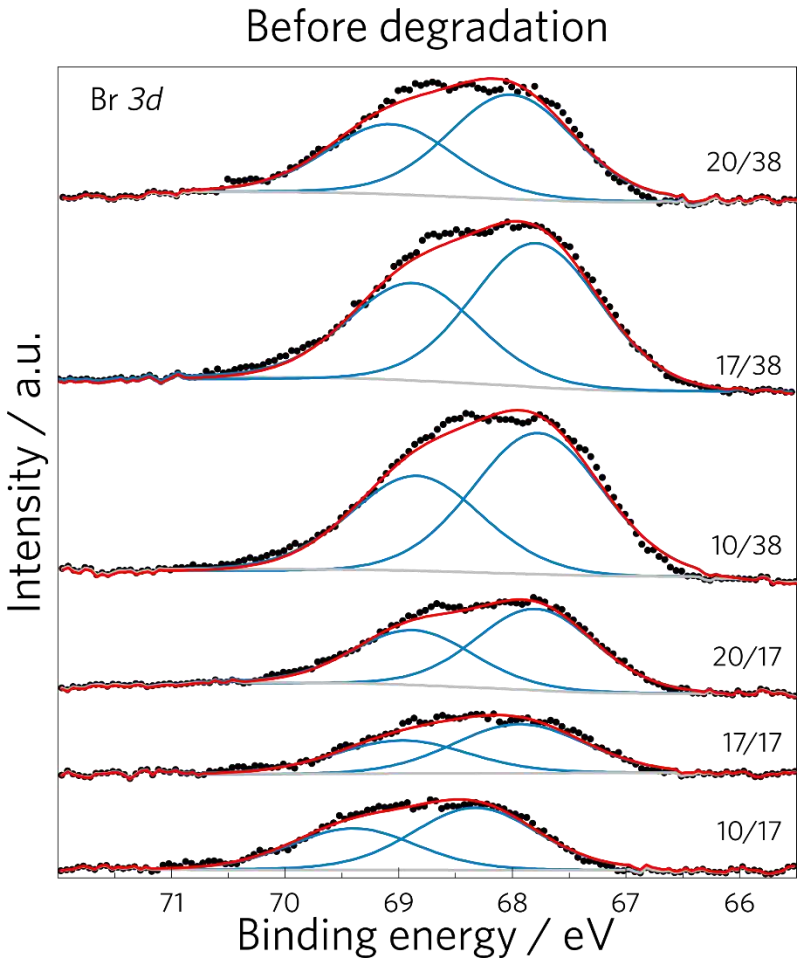

Figure S 15: Hhigh resolution XPS Br 3d core level spectra of pristine samples

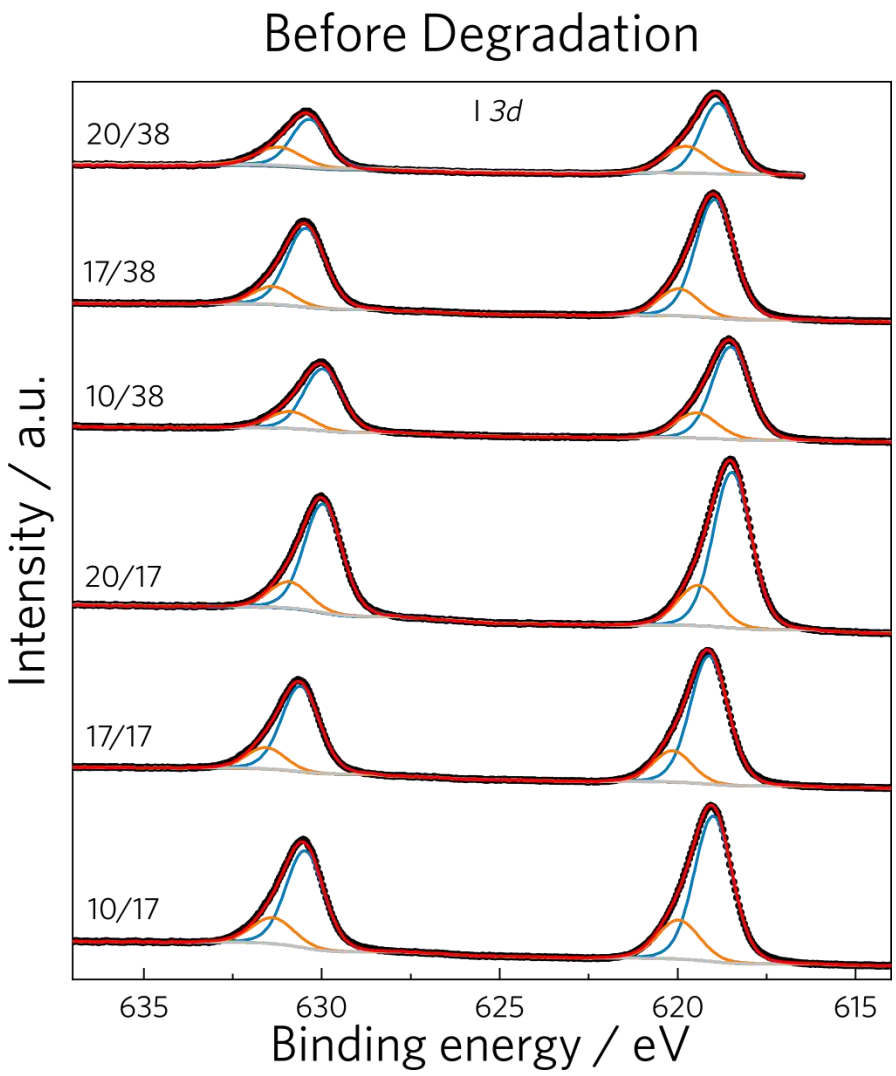

Figure S 16: High resolution XPS I 3d core level spectra of pristine samples.

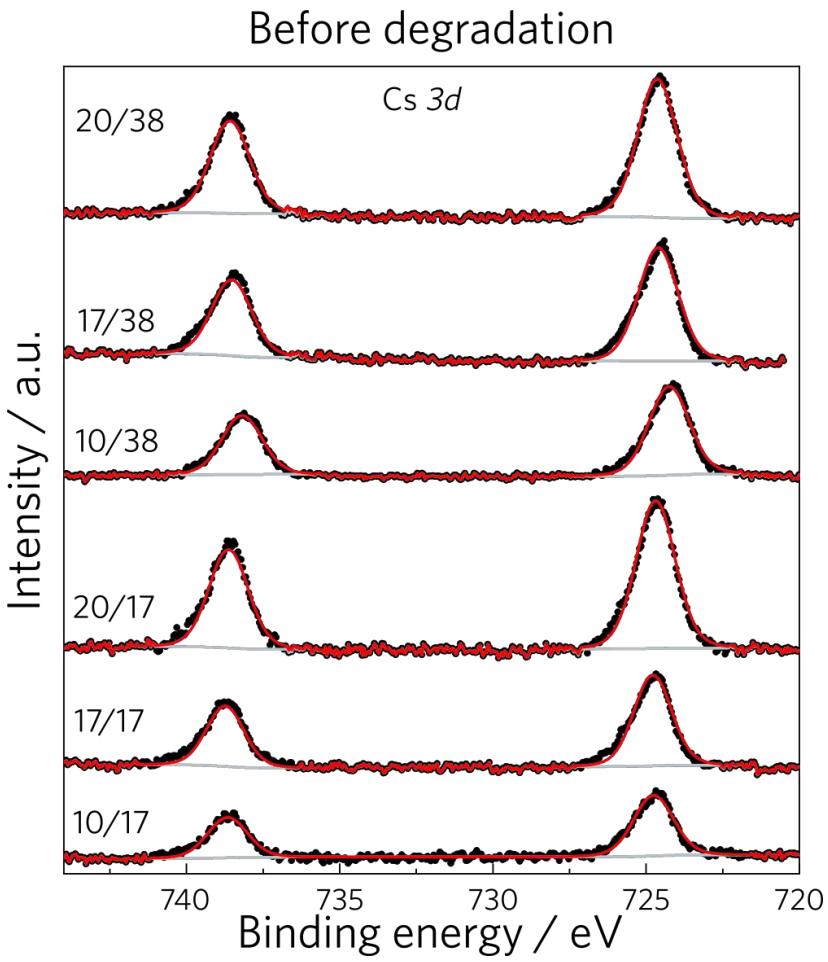

Figure S 17:High resolution XPS Cs 3d spectra of samples of pristine samples .

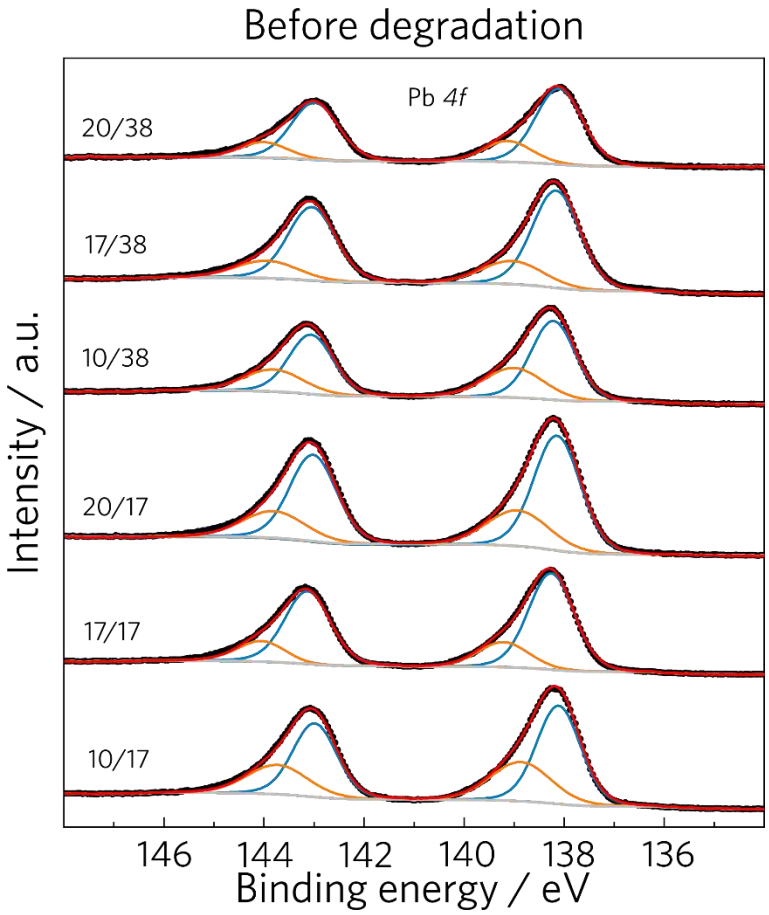

Figure S 18: High resolution XPS Pb 4f core level spectra of samples of pristine samples.

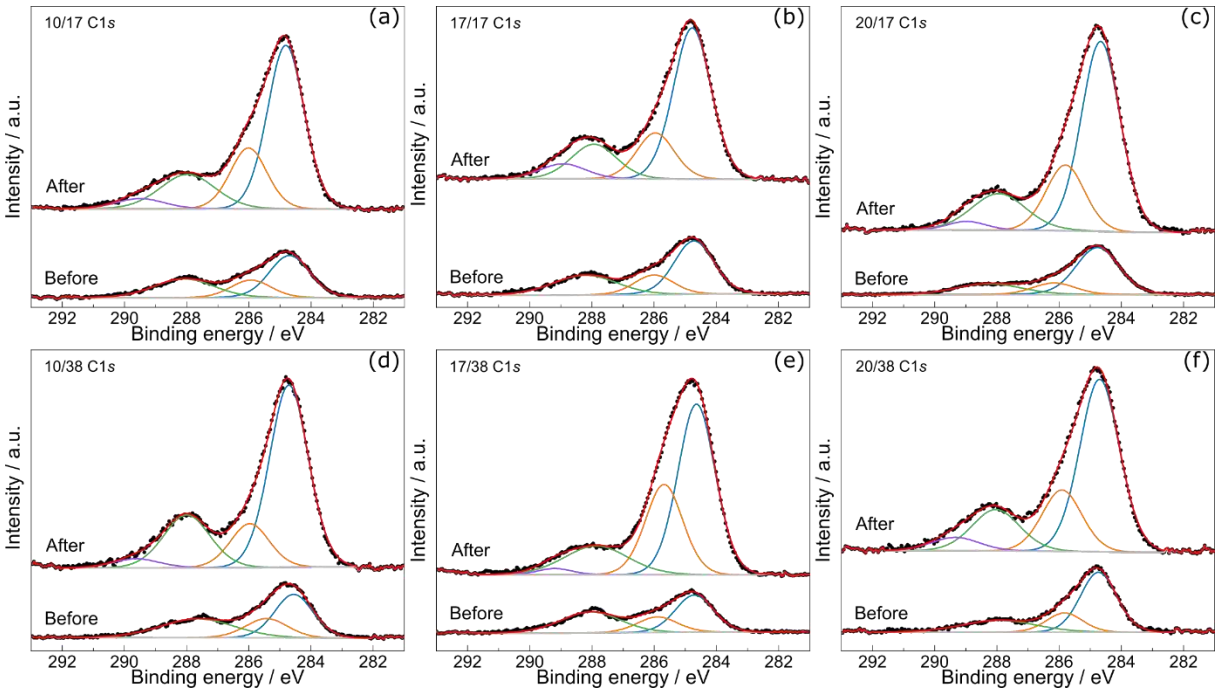

Figure S 19: Before and after degradation high resolution XPS C 1s core level spectra of samples 10/17 (a), 17/17 (b), 20/17 (c), 10/38 (d), 17/38 (e) and 20/38 (f). Deconvolution peaks are attributed to C-H originated from ex-situ absorbed hydrocarbon (blue), C-N bond (orange), conjugated N-C=N (green) and C=O/C-O bond (purple).

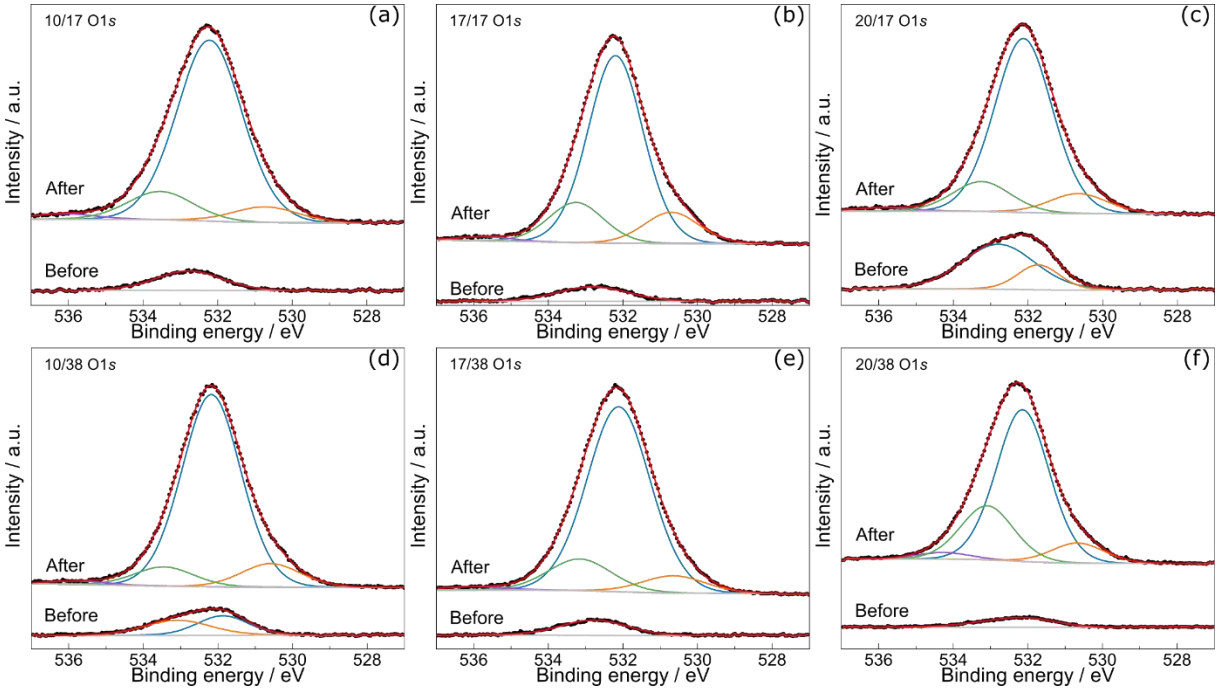

Figure S 20: Before and after degradation high resolution XPS O 1s core level spectra of samples 10/17 (a), 17/17 (b), 20/17 (c), 10/38 (d), 17/38 (e) and 20/38 (f). Deconvolution peaks are attributed to C=O/C-O, carbonate (blue), PbO (orange) O-H bond in $Pb(OH)_2$ (green) and adsorbed H_2O (purple).

Table S 2: Ratio between the deconvolution areas for Br 3d and I 3d high resolution XPS spectra of the degraded samples.

Br 3d Area ratio		
Br(blue)/Br(orange)		
10/17	17/17	20/17
0.8	2.5	1.1
10/38	17/38	20/38
3.4	1.5	0.8
I 3d Area ratio		
I(blue)/I(orange)		
10/17	17/17	20/17
0.3[a]	0.7	1.0
10/38	17/38	20/38
0.6	0.5	0.4

[a] I (orange) area is the sum of orange and green curves in Figure 7(b).

Table S 3: Before and after degradation (Br3d+I3d)/Pb4f and (Br3d+I3d)/Cs3d XPS peak area ratio of the degraded samples.

(Br3d+I3d)/Pb4f	
Before	After

10/17	17/17	20/17	10/17	17/17	20/17
3.2	3.1	3.0	1.9	1.7	1.7
10/38	17/38	20/38	10/38	17/38	20/38
3.6	3.5	3.2	1.5	1.5	1.6
(Br3d+I3d)/Cs3d					
Before			After		
10/17	17/17	20/17	10/17	17/17	20/17
33.7	19.2	15.4	17.8	7.2	6.4
10/38	17/38	20/38	10/38	17/38	20/38
33.3	20.0	12.7	13.6	8.5	6.4

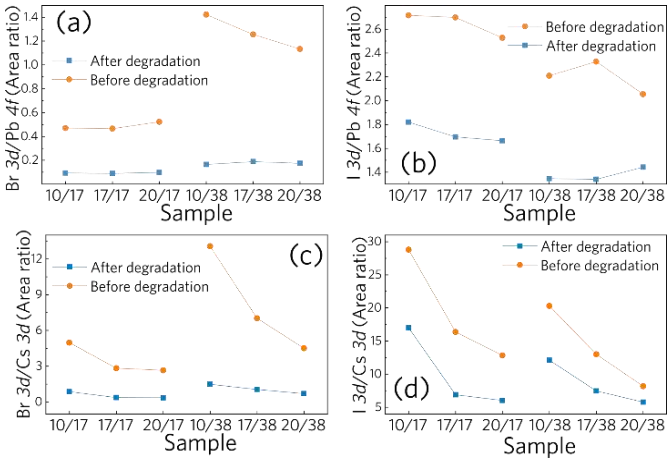

Figure S 21: Ratio of the peak areas from high resolution XPS spectra. (a) Br3d/Pb4f, (b) I3d/Pb4f, (c)Br3d/Cs3d and (d) I3d/Cs3d.

References

[1] P. Gratia *et al.*, "The Many Faces of Mixed Ion Perovskites: Unraveling and Understanding the Crystallization Process," *ACS Energy Lett.*, vol. 2, no. 12, pp. 2686–2693, 2017.

[2] W. Rehman *et al.*, "Photovoltaic mixed-cation lead mixed-halide perovskites: links between crystallinity, photo-stability and electronic properties," *Energy Environ. Sci.*,

vol. 10, no. 1, pp. 361–369, Jan. 2017.

[3] K. Persson, “Materials Data on PbBr2 (SG:136) by Materials Project.” 2016.

[4] F. Chen *et al.*, “Self-Assembled Growth of Ultrastable $CH_3NH_3PbBr_3$ Perovskite Milliwires for Photodetectors,” *ACS Appl. Mater. Interfaces*, vol. 10, no. 30, pp. 25763–25769, Aug. 2018.

[5] J.-W. Lee, D.-H. Kim, H.-S. Kim, S.-W. Seo, S. M. Cho, and N.-G. Park, “Formamidinium and Cesium Hybridization for Photo- and Moisture-Stable Perovskite Solar Cell,” *Adv. Energy Mater.*, vol. 5, no. 20, p. 1501310, Oct. 2015.